Myocardial oxygenation in vivo: optical spectroscopy of cytoplasmic myoglobin and mitochondrial cytochromes

ANDREW E. ARAI,[1] CLAUDIA E. KASSERRA,[1] PAUL R. TERRITO,[1]
AMIR H. GANDJBAKHCHE,[2] AND ROBERT S. BALABAN[1]
[1]*Laboratory of Cardiac Energetics, National Heart, Lung, and Blood Institute, and* [2]*Laboratory of Integrative and Medical Biophysics, National Institute of Child Health and Human Development, National Institutes of Health, Bethesda, Maryland 20892*

Arai, Andrew E., Claudia E. Kasserra, Paul R. Territo, Amir H. Gandjbakhche, and Robert S. Balaban. Myocardial oxygenation in vivo: optical spectroscopy of cytoplasmic myoglobin and mitochondrial cytochromes. *Am. J. Physiol.* 277 (*Heart Circ. Physiol.* 46): H683–H697, 1999.—The oxygenation state of myoglobin and the redox state of cytochrome *c* provide information on the P_{O_2} in the cytosol and mitochondria, respectively. An optical "window" from ~540 to 585 nm was found in the pig heart in vivo that permitted the monitoring of myoglobin and cytochrome *c* without interference from Hb oxygenation or blood volume. Scanning reflectance spectroscopy was performed on the surgically exposed left ventricle of pigs. Difference spectra between control and a total left anterior descending coronary artery occlusion revealed maxima and minima in this spectral region consistent with myoglobin deoxygenation and cytochrome *c* and *b* reduction. Comparison of in vivo data with in vitro fractions of the heart, including Hb-free tissue whole heart and homogenates, mitochondria, myoglobin, and pig red blood cells, reveals minimal contributions of Hb in vivo. This conclusion was confirmed by expanding the blood volume of the myocardium and increasing mean Hb O_2 saturation with an intracoronary infusion of adenosine (20 $\mu g \cdot kg^{-1} \cdot min^{-1}$), which had no significant effect on the 540- to 585-nm region. These results also suggested that myoglobin O_2 saturation was not blood flow limited under these conditions in vivo. Work jump studies with phenylephrine also failed to change cytochrome *c* redox state or myoglobin oxygenation. Computer simulations using recent physical data are consistent with the notion that myoglobin O_2 saturation is >92% under basal conditions and does not change significantly with moderate workloads. These studies show that reflectance spectroscopy can assess myocardial oxygenation in vivo. Myoglobin O_2 saturation is very high and is not labile to moderate changes in cardiac workload in the open-chest pig model. These findings indicate that myoglobin does not contribute significantly to O_2 transport via facilitated diffusion under these conditions.

oxygen; mitochondria; oxygen consumption; facilitated diffusion; pig; dog; cytochrome *b*; cytochrome *c*; diffusion; computer simulation; hemoglobin

THE LABILE VISIBLE LIGHT absorption of the heart in vivo is mostly dependent on the oxygenation status of myoglobin and Hb, the redox state of the cytochromes, and myocardial blood volume. Thus the reflectance spectroscopy can monitor each of these important parameters in myocardial O_2 transport. Although visible optical spectroscopy has been used to study the perfused heart, papillary muscles, and isolated myocytes (6, 12, 19, 20, 28, 42, 46), less work has been attempted on the heart in vivo (5, 25, 29, 34, 35, 39, 40, 43). Four factors make it difficult to use reflectance spectroscopy on a beating, blood-perfused heart: *1*) motion artifacts, *2*) changes in blood volume, *3*) spectral overlap between absorption of myoglobin, Hb, and the cytochromes, and *4*) limited depth of light penetration. Infrared spectroscopy has been used to overcome the limited path length but requires multicompartmental modeling to quantify changes in Hb oxygenation and content, making the residual measures of myoglobin oxygenation and cytochrome redox state difficult (34, 35).

In preliminary studies the band at ~560 ± 20 nm of the reflected optical spectrum appeared to be largely insensitive to absorbance changes related to Hb oxygenation and blood volume changes. The hypothesis was generated that this "window" in the optical spectrum is not significantly influenced by Hb, permitting the direct detection of cytochromes and myoglobin. To test this hypothesis, comparisons between in vivo heart optical spectra with and without blood as well as in vitro porcine blood and blood-free myocardial homogenates were performed. Studies were also performed on porcine hearts in vivo during normal perfusion, ischemia, and adenosine-induced coronary vasodilation to evaluate the effects of changes in blood volume and Hb oxygenation. Finally, studies were conducted on the effect of increased workload on myocardial oxygenation. Computer simulations of O_2 delivery to the myocardium were also performed using recent functional and morphological data.

A secondary hypothesis was generated that the lack of Hb influence was due to the short path length caused by the high optical absorption of tissue chromophores and the low capillary content of red blood cells (RBCs). This second hypothesis is developed further in the companion article (15).

MATERIALS AND METHODS

Animal preparation. All animal care research protocols were approved by the Animal Care and Use Committee at the National Institutes of Health and conform to the standards of the American Physiological Society. Domestic swine of either gender, weighing 25–55 kg, were studied in an acute open-chest preparation. Animals were premedicated intramuscularly with ketamine, xylazine, and butorphanol (Torbugesic). Anesthesia was induced with α-chloralose (10 g/l) at a dose of 10–15 ml/kg iv. Anesthesia was maintained with 5–10 ml/kg

The costs of publication of this article were defrayed in part by the payment of page charges. The article must therefore be hereby marked "*advertisement*" in accordance with 18 U.S.C. Section 1734 solely to indicate this fact.

iv boluses every 1–2 h as needed or, in some animals, by a heated continuous infusion at 5–10 $ml \cdot kg^{-1} \cdot h^{-1}$ to maintain adequate anesthesia. Ventilation was provided by a hospital-grade servoventilator (model SV900, Siemens). Acid-base status and blood gases were monitored. The arterial pH was maintained between 7.35 and 7.45 by adjusting the ventilator or giving intravenous bicarbonate. The P_{O_2} was maintained at >100 mmHg. Body temperature was maintained by keeping the operating room temperature elevated (30–32°C) with a heated water blanket and Mylar heat-reflecting blankets.

Initial anesthesia was given through an ear vein catheter. Large-bore catheters were then placed in the femoral artery and vein. A midline thoracotomy was performed, and the heart was suspended in a pericardial cradle. The left anterior descending coronary artery (LAD) was dissected, and a hydraulic occluder was placed around the proximal portion of the vessel above the occlusion site. A transit-time ultrasound flow probe was placed around the middle of the LAD (model T201 2-channel ultrasonic blood flowmeter, Transonics Systems, Ithaca, NY). A 6-Fr catheter-tipped manometer (Millar, Houston, TX) was introduced into and sutured to the left ventricular (LV) apex by way of a short 7-Fr introducer with side port. In animals receiving intracoronary adenosine, a 26-gauge Angiocath was placed in a right ventricular branch of the LAD or the main LAD if no side branch was available.

The basic work jump protocol was an increase in cardiac work followed by a local LAD infusion of adenosine and then total LAD occlusion. Recovery periods (30–45 min) were spaced between interventions. Phenylephrine (6 $\mu g \cdot kg^{-1} \cdot min^{-1}$ iv for 7 min) was used to study the effects of an increase in cardiac work on myoglobin oxygenation. Adenosine (20 $\mu g \cdot kg^{-1} \cdot min^{-1}$ for 7 min) and total LAD occlusion were used to estimate the physiological dynamic range of the oxygenation effects in each animal as well as the effects of Hb oxygenation and blood volume. Control data were acquired for ~2.5 min before the phenylephrine infusion. Spectra were then collected continuously through the infusion protocol. In some animals it was necessary to repeat the phenylephrine dose after repositioning of the optics because of heart movement that placed the aperture mask out of the field of illumination (see below). After proper adjustment of the optics, the aperture remained in the illumination field throughout the control and experimental periods.

In a subset of animals the spectral effects of blood removal on the ischemia difference spectrum were evaluated in the intact heart. Animals were also fitted with an inflatable occluder placed proximal to the first distal branch of the LAD, allowing generation of transient reversible ischemia. Control blood-perfused spectra were collected at an acquisition rate of 100 ms for 3 min, and then ischemia was initiated for an additional 3 min. No cardiac gating was used in these studies. Reperfusion spectra were also collected after occlusion to ensure restorative myocardial oxygenation. After reperfusion the superior and inferior vena cava were ligated distal to the base and apex, respectively, and a 1-cm-long right atrial vent was placed between the ligatures. Cardioplegia was initiated by passing ice-cold (2°C) buffer (153 mM NaCl, 16 mM $MgSO_4$, and 16 mM KCl equilibrated with 100% O_2) at 200 mmHg through a 14-gauge needle, which was inserted into the ascending aorta after cross clamping. Evacuated fluids were aspirated to minimize cross contamination of blood on the surface of the heart. The clearance of the blood was evaluated from observation of the venous effluent from the heart. Oxygenated myocardial blood-free spectra in situ were obtained as described for control blood-perfused animals in the cold-arrested heart. Ischemia spectra were collected by allowing the tissue to warm and collecting data at 10-min intervals until a stable ischemia spectrum was obtained. In all cases, felt and dark current spectra were obtained for computation of corrected optical density (OD).

Reflectance spectroscopy. Localized reflectance spectroscopy was measured as shown in Fig. 1. A black felt mask (~25 cm^2) was spot glued, with care taken to avoid obvious surface vessels, with *n*-butyl cyanoacrylate (Vetbond) adhesive to the distal anterior LV myocardium in an area predicted to be served by the LAD on the basis of surface diagonal branches. A round ~1-cm hole was cut out of the middle of the felt mask. This mask served to localize the measurements to one discrete portion of the myocardium. Regions free of obvious epicardial fat and blood vessels were selected during positioning of the mask. Illumination light was from a high-intensity tungsten source. A small fraction of the output was selected by an integrating sphere and projected onto the heart. The amount of light was adjusted to optimize the dynamic range of the detector. The projection and detection optics were in a nonconfocal arrangement and oriented obliquely relative to

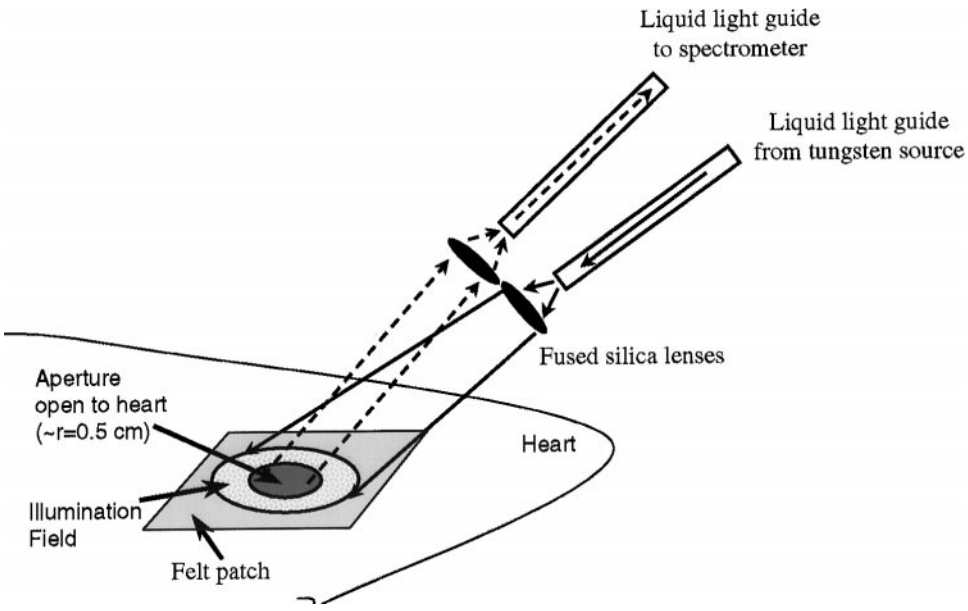

Fig. 1. Schematic diagram of optical illumination and detection system. Black felt aperture was glued to myocardium to ensure that only one selected region of myocardium was analyzed. Large vessels were avoided in aperture. Illumination and detection area was roughly twice radius (*r*) of aperture to minimize effects of in-plane motion on spectrum of reflected light.

the surface of the heart to minimize specular reflections. Illuminating and detecting from a larger region around the aperture in the mask ensured that the entire region of interest was always detected. This greatly minimized translational motion-related artifacts as well as concerns regarding heterogeneity of the surface optical properties. Theoretically, motion should cause intensity shifts because of changes in angle of incident light, with no changes in the spectral characteristics. All data were ratiometrically corrected for any spectral characteristics of the black felt mask and detector with the use of a felt reference spectrum. All changes in OD (ΔOD) reported were calculated by subtracting the logarithm of reflected light under experimental conditions from the logarithm of the reflected light under control conditions. This is equivalent to the −log(experimental condition/control).

The reflected light was concentrated into a liquid light guide, with the distal end placed at the 0.1-mm slit of a 0.32-m Czerny-Turner spectrometer (model HR320, Instruments SA). Spectra were detected by an ultraviolet light-enhanced 512-element scanning photodiode array (EG & G PARC, Princeton, NJ). Spectra were collected from 385 to 640 nm. The data were collected in blocks of 34 spectra at 20 Hz, repetitively triggered by the cardiac R wave. Spectra from 16 blocks were averaged to produce 30- to 45-s time resolution data depending on the heart rate. Time course or cardiac cycle data were extracted by sorting the data in memory.

There was a theoretical concern that the impinged light could affect the resting temperature of the epicardium, which could alter the physiology and myoglobin O_2 affinity (38). Epicardial temperatures were obtained via a hypodermic microprobe (model MT-26/2, Physiotemp, Clinton, NJ) implanted just under the subepicardial surface or placed on the surface of the heart. Temperature was monitored using a calibrated voltage source (model BAT-12, Physiotemp). Direct measures of temperature were collected at 0.2 Hz for 30 min with and without the tungsten-halogen source at full power. The central core temperature measured rectally was regulated, using the water jacket and room temperature, to 37.1 ± 0.2°C. The surface temperature of the heart averaged 36.7 ± 0.02°C without the light and 36.8 ± 0.01°C with the light. These data suggest that the heat capacity of the blood-perfused heart was more than adequate to dissipate the heat load from the light.

Spectral fitting. The linear least-squares methodology follows from the previous work of French et al. (13). Spectral fitting was performed using a linear least-squares fitting routine resident in the SigmaPlot (Jandel) software package. Fits were evaluated from the R^2 values as well as visual inspection of the frequency dependence of the residuals.

Blood flow measurements. Fluorescent microsphere blood flow was measured in a subset of animals. Approximately $2–2.5 \times 10^6$ E-Z Trac microspheres were injected into the left atrium before and during a given experimental perturbation. Different-color spheres were used for each measurement. Reference blood samples (20 ml) were obtained from the femoral vein at a rate of 10 ml/min during each injection. At the end of the study, myocardial samples taken from the LAD zone and the non-LAD zone were quantified through the E-Z Trac Investigator Partner Services (Interactive Medical Technologies, Los Angeles, CA).

Tissue samples. Triton X-100-solubilized pig heart homogenate was prepared as previously described (1). Briefly, animals were anesthetized and surgically prepared as discussed above, except for instrumentation on the heart itself. The animals were heparinized, and the hearts were rapidly removed. The hearts were then immediately perfused in a retrograde fashion via aortic cannulation with ice-cold saline until no evidence of blood was apparent in the effluent (1–2 liters of perfusate). Samples (5–10 g) of the free LV wall were then dissected free of fat and connective tissue and finely minced over ice. This sample was then homogenized in an equal weight of 100 mM phosphate buffer (pH 7.1). Care was taken not to heat the sample to prevent the formation of metmyoglobin. Aliquots of this homogenate were dissolved 1:5 in Triton X-100 to solubilize the tissue. Solid material was removed by gentle centrifugation, and the supernatant was used as a blood-free homogenate of porcine heart. Isolated pig heart mitochondria and Triton X-100 extracts were prepared as described by Mootha et al. (30).

Myoglobin determination. Hb-free tissue extracts of the pig heart were used to determine the concentration of myoglobin. Samples were split into two 1-ml aliquots. One sample (reference sample) was supplemented with 10 mM sodium ascorbate and 200 μM NaCN to reduce cytochromes *c* and *a* (1). The remaining sample (experimental sample) was completely deoxygenated and reduced using $Na_2S_2O_4$. Difference spectra between the reference and experimental samples were collected from 450 to 620 nm on a scanning spectrophotometer (Perkin-Elmer). The reduced cytochrome *a* in the reference and the experimental sample resulted in only myoglobin contributing to the difference spectrum in the 595- to 620-nm region. Thus the concentration of myoglobin was determined by the absorbance difference between 595 and 620 nm in these difference spectra.

The extinction coefficient for horse myoglobin (Sigma Chemical, St. Louis, MO) at these wavelength pairs in oxygenated-deoxygenated spectra was determined on the same instrument. A myoglobin stock solution was first completely reduced by titration with $Na_2S_2O_4$. The progress of the titration was followed optically. The reduced myoglobin was oxygenated by exhaustive room air bubbling. Samples were prepared with oxygenated and deoxygenated (retreated with $Na_2S_2O_4$) myoglobin and run in a differential mode on the spectrophotometer. Protein concentrations from 0.2 to 0.8 mg/ml were measured, and the extinction coefficient for the difference between 620 and 595 nm ($\Delta OD_{620-595}$) in the oxygenated deoxygenated myoglobin was determined to be $4{,}715\ \Delta OD_{620-595} \cdot cm^{-1} \cdot M^{-1}$ with a molecular weight of 16,900.

RESULTS

In vivo cardiac ischemia: control difference reflectance spectra. Control and ischemia reflectance spectra and the corresponding difference spectrum from an in vivo pig heart are shown in Fig. 2, *A* and *B*. The minimal changes below 435 nm are presumably due to the high tissue absorbance at these wavelengths. At longer wavelengths, calculated ΔOD is negative (less absorbance during ischemia). This was observed in most of the ischemia studies. This systematic effect appears associated with the swelling of the LV surface closer to the detector during ischemia. In contrast to previous work on perfused hearts during the transition from hypoxia to oxygenation, the physiological constraints of the in vivo beating heart eliminated the ability to hold the heart relative to the optics, resulting in the normal isobestic points being nonzero. Spectral absorbance differences are best observed from control-ischemia reflectance ΔOD spectra (Fig. 2*B*). Minima in the ΔOD spectrum correspond to the maximal decreases in absorbance, which occur at 480, 535, and 582

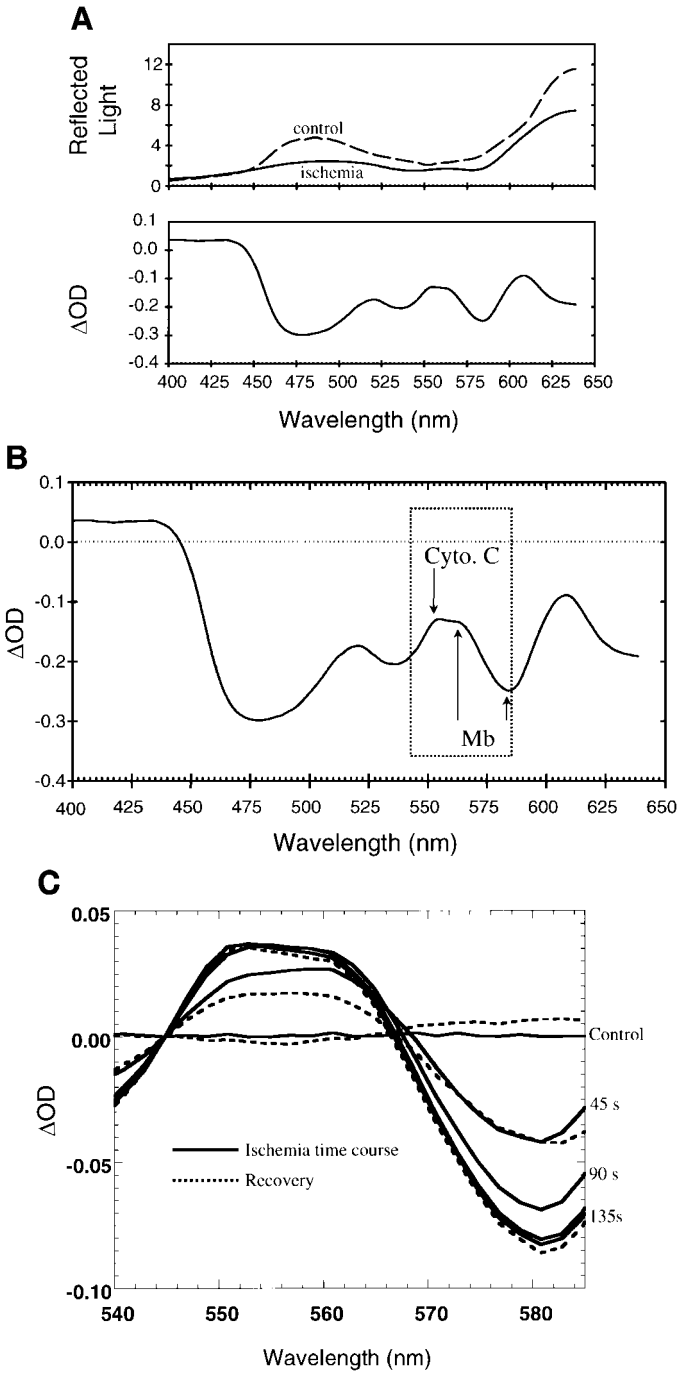

Fig. 2. In vivo reflectance spectra from pig heart. *A*: absolute intensity and change in optical density (ΔOD) spectrum from a pig heart. ΔOD = log(control) − log(ischemia). *B*: expanded ΔOD spectrum from *A*. Cyto *c*, cytochrome *c*; Mb, myoglobin. *C*: ΔOD time course during ischemia and recovery. Spectra were collected continuously (45-s resolution) through an ischemia-and-recovery procedure. Ischemic period was ~225 s. ΔOD was calculated as log(initial control spectrum) − log(time point). First ΔOD spectrum was calculated from 2 initial control spectra. Data were normalized to 545 nm isobestic (21) to minimize baseline effects.

nm. Maxima in the spectrum were at 520, 550, 563, and 605 nm.

A representative time course of difference spectra during an ischemia-recovery protocol is shown in Fig. 2*C*. The data are normalized to the 545-nm isobestic wavelength, determined in Hb-free perfused rabbit hearts (21), to minimize the baseline effects. The selection of this isobestic wavelength reasonably maintains the other isobestic point in this spectrum at 568 nm, also determined in blood-free perfused rabbit hearts. The time resolution of 45 s was limited by the acquisition schemes in the scanner and not the signal-to-noise ratio of the measurements.

The maxima, minima, and isobestic points in the ΔOD spectra are not at the wavelengths expected for changes in Hb content or Hb O_2 saturation. Thus we attempted to determine the tissue chromophores contributing to this spectrum. Toward this goal, the in vivo ΔOD data were compared with in vitro data collected from several fractions of heart, as summarized in Fig. 3. Blood-free pig myocardial homogenates were used to represent total tissue chromophores, isolated porcine mitochondria for the mitochondrial chromophores, purified horse myoglobin for cytosolic myoglobin, and pig RBCs/Hb for blood constituents. In general, difference spectra were collected with and without $Na_2S_2O_4$ to remove O_2 and reduce cytochromes. Normalized spectra are presented for the blood-free homogenate representing all cellular chormophores, cytochromes, and myoglobin in the naturally occurring ratio of concentrations. Blood-free pig myocardial homogenates treated with KCN (0.2 mM) and sodium ascorbate (5 mM) selectively reduced cytochrome *c* at 550 nm and cytochrome a,a_3 at 605 nm (1). Purified myoglobin deoxygenation spectra have maxima at 563 nm and minima at 581 nm. Cytochrome *b* has a deoxygenation absorbance peak at 563 nm when blood-free, myoglobin-free mitochondrial suspensions are reduced with $Na_2S_2O_4$.

By visual inspection the in vivo ischemic ΔOD spectrum corresponded most closely with the $Na_2S_2O_4$ ΔOD

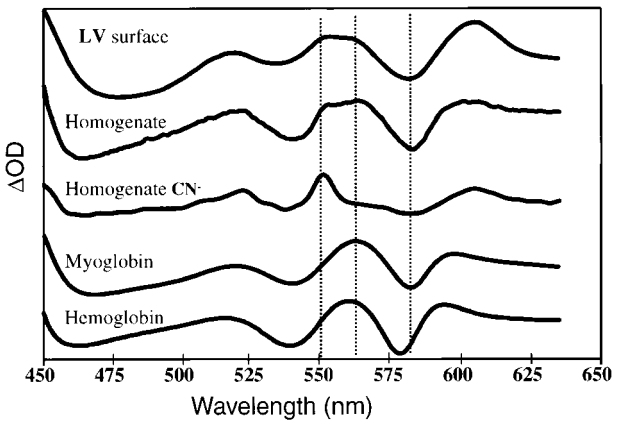

Fig. 3. Representative ΔOD spectra from in vivo heart and several in vitro samples. In general, ΔOD spectra were generated in in vitro samples by subtracting logarithm of Na_2SO_4-treated sample spectra from logarithm of control spectra. No *y*-scale is provided, because this was highly variable among different preparations and only spectral shape was used in this analysis. Dotted lines are presented to guide eye at 581, 563, and 551 nm, which discriminate Hb, myoglobin, and cytochrome. One exception is tissue extract that was treated with cyanide and ascorbate to reduce cytochrome *c* and cytochrome oxidase alone. In this case, logarithm of cyanide-treated sample spectrum was subtracted from logarithm of control spectrum. LV, left ventricle.

spectrum of the blood-free myocardial homogenate. The shoulder at 550 nm corresponds to cytochrome *c*. The minimum at 581–582 nm corresponds to the myoglobin deoxygenation not the minimum of pig blood Hb at ~577 nm. Qualitatively, the relative maximum and relative minimum observed in vivo correspond within 1 nm of the individual components identified in the in vitro experiments. These data are consistent with the hypothesis that the in vivo ischemia absorbance changes in the 540- to 585-nm region are dominated by the cellular chromophores, mitochondrial cytochromes, and cytoplasmic myoglobin.

The extent to which Hb contributes to the in vivo ischemia-related absorbance changes was evaluated quantitatively by intentionally contaminating blood-free tissue homogenates with pig blood and monitoring the spectral minimum in the 580-nm region. The in vivo spectra demonstrate a relative minimum in the ischemia-to-control ratio spectrum at 581.9 ± 0.9 nm ($n = 6$). In vitro deoxygenation absorbance spectra of blood-free myocardial homogenates had a minimum at 581.3 ± 0.7 nm ($n = 5$) that was not significantly different from that in vivo ($P > 0.05$, *t*-test). Titration of extract minima with pig Hb is presented in Fig. 4. The minimum frequency was very sensitive to Hb contamination. Contaminating the blood-free myocardial homogenate with the equivalent of ~0.3% RBC by volume shifted the minimum to 579.1 ± 1.0 nm, which was significantly different from the pure homogenate ($P < 0.05$, paired *t*-test). Approximately 1% contamination of myocardial homogenate with RBC shifted the minimum even closer to that of pure blood (577.0 ± 0.2 nm, $P < 0.01$, paired *t*-test). Thus ~0.3% RBC volume contamination would be predicted to start shifting the position of this minimum by ~1–2 nm, which could be detected in the in vivo spectra. It is also important to note that blood contamination of >0.5% RBC volume resulted in complete masking of the cytochrome *c* shoulder at 550 nm (not shown), further supporting the notion that the blood contamination was very small. These data indicate that absorption changes associated with ischemia in vivo represent primarily myoglobin and the cytochromes with very little contribution from Hb. The potential reasons that Hb is not detected are reviewed in DISCUSSION.

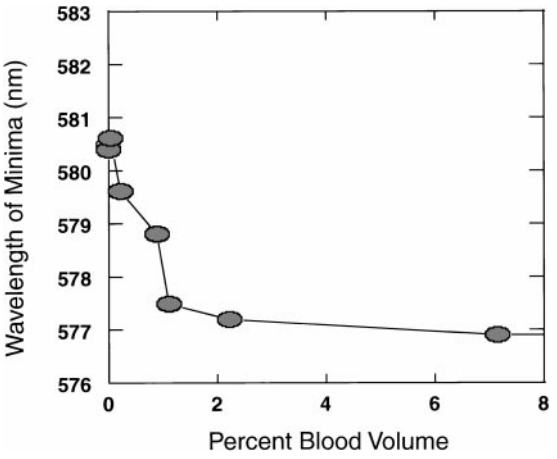

Fig. 4. Effect of added porcine blood on $Na_2S_2O_4$ ΔOD spectral minima in 580-nm region of Hb-free heart extracts. Percent blood is on a volume-to-volume basis. Zero percent points are for tissue extracts in absence of red blood cells.

Spectral fitting. To attempt to quantify the contributions of cytochromes and myoglobin to the in vivo ischemia spectra, linear least-squares routines were used to fit the in vivo data. Two analyses were performed. The first involved fitting a combination of in vitro mitochondria and myoglobin (Fig. 5) difference spectrum to the in vivo ischemia difference spectrum. With use of the following equations, a linear least-squares fit of *Eq. 3* to the in vivo spectra was performed

$$A_{\text{mito}} = \text{I}_{\text{mito}}\text{OD}_{\text{mmito}} + C_1 \quad (1)$$

$$A_{\text{Mb}} = \text{I}_{\text{Mb}}\text{OD}_{\text{mMb}} + C_2 \quad (2)$$

$$\text{f} = A_{\text{mito}} + A_{\text{Mb}} \quad (3)$$

where OD_{mmito} and OD_{mMb} are the mitochondria and myoglobin model ischemia ΔOD spectra collected in vitro, I_{mito} and I_{Mb} are the relative amplitudes of the mitochondrial and myoglobin contributions, C_1 and C_2 are constants, and A_{mito} and A_{Mb} are the amplitude-adjusted mitochondria and myoglobin absorbance spectra that, in combination, provided the best fit (f) to the in vivo spectrum. The models used and the results of the spectral fitting routine are presented in Fig. 5. Good fits of the in vivo data with the mitochondria-myoglobin model were obtained using this approach with minimal residuals ($R^2 = 0.97 \pm 0.03$, $n = 6$). The $\text{I}_{\text{Mb}}/\text{I}_{\text{mito}}$ ratio for the models used was 29.4 ± 3.0 ($n = 5$) for in vivo spectra and 29.3 ± 1.0 ($n = 4$) for the blood-free Triton X-100 extracts. The similarity of in vivo and in vitro $\text{I}_{\text{Mb}}/\text{I}_{\text{mito}}$ ratios suggests that the relative amounts of myoglobin and mitochondria chromophores are the same in the blood-free extracts and in vivo. To confirm this, the in vitro blood-free homogenate spectrum was the only model system used to fit the in vivo data with the same linear least-squares strategy. The single blood-free homogenate spectrum was found to be very similar ($R^2 > 0.96$, $n = 5$) to the in vivo spectrum. Fits using Hb alone or Hb and mitochondria model spectra resulted in consistently lower R^2 values. These results support the hypothesis that the Hb contamination to the in vivo optical spectrum was minimal and that spectral contributions from cytochrome *c* and myoglobin alone, in the relative concentrations found in tissue extracts, were adequate to fit the in vivo data in this spectral region.

As a further control, the ischemic ΔOD spectrum of the intact heart with and without blood was evaluated. In Fig. 5*B*, the ischemic ΔOD spectra of the same heart perfused in situ with blood and thoroughly perfused with cardioplegia solution are presented. A linear regression was also performed in the region from 540 to 615 nm between the two data sets to quantitatively evaluate the shape differences of the spectra. The absorption minimum at ~580 nm is maintained along with the cytochrome shoulder at ~550 nm in both spectra. The linear regression in the 540- to 585-nm window showed

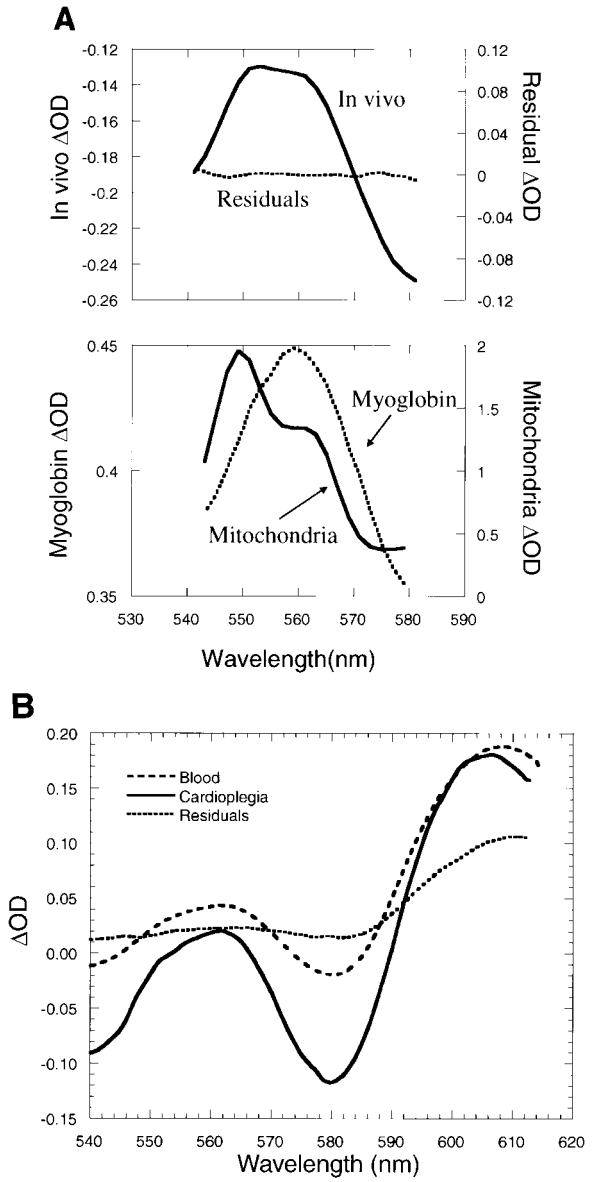

Fig. 5. *A*: linear least-squares fit of in vivo ischemia difference spectrum with combined model spectra from pig heart mitochondria and horse myoglobin. *Bottom*: model ischemic ΔOD spectra of mitochondria and myoglobin. These spectra were combined as described in *Eqs. 1–3*. Amplitudes of spectra were varied to result in a minimum residual compared with in vivo spectrum. *Top*: in vivo ischemia ΔOD spectrum and residuals of model fit. *B*: ischemic difference spectra from a pig heart in presence and absence of blood. In vivo control-ischemia data were collected using our standard procedures. Heart was then rapidly perfused with cold cardioplegia medium to maintain oxygenation. Control spectra were collected that were stable for >20 min. Ischemia spectra were collected after partial rewarming to room temperature. Complete ischemic state was assumed to occur when a stable spectrum was maintained for >10 min. ΔOD spectra were calculated as described above. A linear regression between in vivo and blood-free ischemia ΔOD spectra was performed, and residuals of this comparison are also shown. Data beyond 585 nm are presented to show that effects of blood removal can be observed at these wavelengths.

minimal residuals with $R^2 > 0.99$. Beyond the 585-nm point the absorbance differences between the conditions increased as the tissue absolute absorbance decreased and effective optical path length through the tissue increased (Fig. 5*B*). These data confirm that the ΔOD spectrum between 540 and 585 nm is minimally perturbed by tissue Hb content. However, above this window, significant differences in the ischemic difference spectrum are observed between blood-perfused and blood-free tissue.

Effects of motion on reflectance spectrum. The felt mask is intended to ensure that only light coming from the open aperture is collected for analysis. This ensured that the same region of the myocardium was evaluated during the experimental perturbations, minimized the inclusion of large surface blood vessels, and reduced the influence of translational motion on the amplitude of the reflected signal. By illuminating a region on the felt mask larger than the open aperture, the open aperture was evenly illuminated and detected. Amplitude variations still occurred as a result of the heart moving closer to or farther from the optics and changes in the angle of incidence of the light with the rotation of the heart. An example of a motion-related artifact is shown in Fig. 6, where the signal intensity at five wavelengths is plotted as a function of time after an R wave trigger. The amplitude variation across the cardiac cycle is on the same order of magnitude as the ischemia-specific absorbance changes. However, the relative spectral characteristics of the light are unchanged in several spectral bands. All wavelengths between 540 and 585 nm have similar time courses, whereas 592 nm is equal in intensity to the other wavelengths at some times but at other times deviates significantly. This is demonstrated spectrally at six phases of the cardiac cycle ranging from midsystole to late diastole in Fig. 7. Despite baseline offsets, the spectra remain flat across the cardiac cycle from 540 to 585 nm but not at longer wavelengths such as 592 nm. Thus cardiac motion does not introduce spectral changes in the 540- to 585-nm region, despite large amplitude offsets introduced by respiratory and cardiac motion.

Epicardial myoglobin oxygenation. The oxygenation status of myoglobin and the redox state of the cytochromes were evaluated in vivo by comparing ischemia

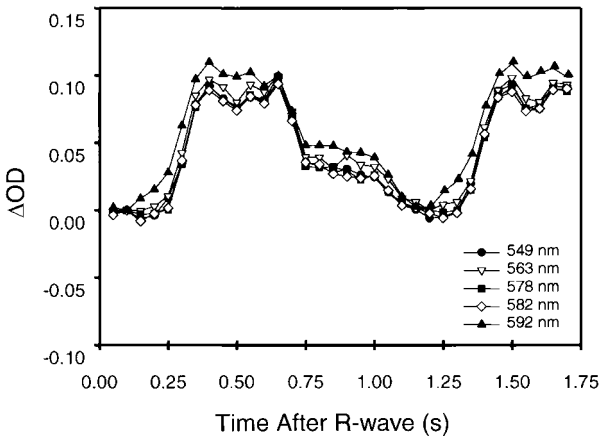

Fig. 6. Reflected light intensity as a function of time after an R wave at 5 different wavelengths. ΔOD was calculated as logarithm of amplitude at *time 0.00* at given wavelength − logarithm of different time points.

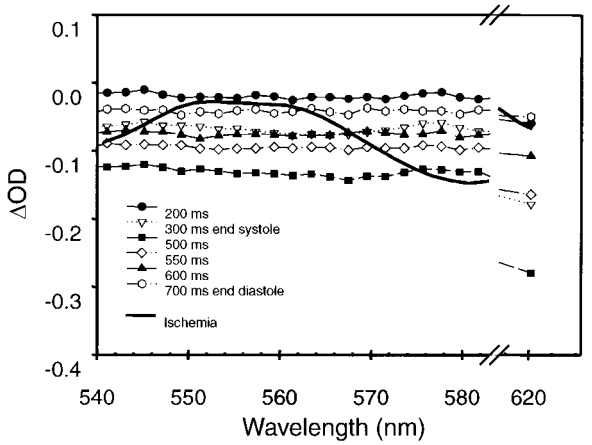

Fig. 7. ΔOD spectra of reflected light at different phases of cardiac cycle. ΔOD was calculated as logarithm of *time 0.0* spectrum − logarithm of spectra collected at indicated times in cardiac cycle. A ΔOD spectrum for ischemia is provided for reference. ΔOD spectrum for ischemia was calculated as described in Fig. 2.

and adenosine experiments. Full-scale deoxygenation of myoglobin and reduction of the cytochromes were defined by the absorbance changes after 2.5 min of total LAD occlusion in the beating heart. Full-scale oxygenation of myoglobin was defined by near-maximal coronary vasodilation achieved by intracoronary adenosine infusion (20 $\mu g \cdot kg^{-1} \cdot min^{-1}$). An example of the reflectance spectra and the absorbance change spectrum associated with myocardial ischemia is shown in Fig. 2. During ischemia, ΔOD between 581.5 and 559 nm ($\Delta OD_{581.5-559}$), a wavelength pair-sensitive myoglobin oxygenation, was only −0.046 ± 0.036. This represents a maximal amplitude change associated with the deoxygenation of myoglobin. In contrast, near-maximal coronary vasodilation with intracoronary adenosine (coronary blood flow was 2.9 ± 0.6 times control, Table 1) had a minimal effect on the reflectance spectra (Fig. 8) within the bandwidth from 540 to 585 nm. On average, $\Delta OD_{581.5-559}$ was only +0.001 ± 0.004 during adenosine infusion ($P < 0.05$ vs. ischemia, paired *t*-test, $n = 6$). Thus adenosine did not significantly change absorbance at wavelength pairs maximally sensitive to the oxygenation status of myoglobin. Because of the lack of spectral response to adenosine, the linear least-squares analysis was not performed. These data indicate that myoglobin is fully oxygenated within the limits of this measurement technique and under these experimental conditions. Hemodynamic characteristics are summarized in Table 1. In paired experiments on animals with this instrumentation and anesthesia ($n = 8$), coronary venous P_{O_2} averaged 23.1 ± 2.1 mmHg and varied by <1.6 mmHg across multiple interventions. In addition, hematocrit averaged 29.2 ± 3.1 for these young animals and was stable across time.

Effect of myocardial workload. The hemodynamic results for the phenylephrine protocol are presented in Table 1. Optical spectra for the phenylephrine study are summarized in Fig. 9. The difference between 559 and 581 nm in the control vs. phenylephrine infusion was not significant at 0.003 ± 0.002 ΔOD (paired *t*-test, $n = 6$).

Myoglobin concentration. The myoglobin concentration in the pig heart was determined because of the discrepancies in the literature. The elimination of blood and cytochrome contamination is critical in any optical assessment of myoglobin in heart tissue. In Fig. 10, difference spectra for $Na_2S_2O_4$-treated vs. raw extract, which will have a myoglobin and a cytochrome contribution, and $Na_2S_2O_4$-treated vs. cytochrome-reduced (KCN and sodium ascorbate treatment) extract, which should have only myoglobin contributions, are presented for comparison. The extract was devoid of a significant contribution from Hb on the basis of the difference spectra minimum at 581 nm (see above). The contribution of cytochrome to the difference spectrum was minimized by the prior reduction of the cytochromes. This was best seen as the removal of the cytochrome *c* shoulder at 550 nm and the shift of the absorbance maximum in the 600-nm region from a mixture of cytochrome *a* and myoglobin to pure myoglobin at 595 nm. The 595-nm peak was used to avoid contamination from cytochrome *b* that is not fully reduced by the cyanide-ascorbate treatment.

The concentration of myoglobin in the pig heart was determined to be 6.1 ± 0.6 ($n = 3$) g/kg wet wt or ~360 μmol/kg (myoglobin molecular weight assumed to be 16,900). This was based on the wavelength pair 595 and 620 nm and the experimentally determined extinction coefficient.

Table 1. *Hemodynamic parameters in phenylephrine protocol*

Procedure	Systolic Pressure, mmHg	Diastolic Pressure, mmHg	LV Systolic Pressure, mmHg	−dP/d*t*, mmHg/s	+dP/d*t*, mmHg/s	Coronary Blood Flow, ml/min
Phenylephrine						
Control	86 ± 15	46 ± 9	88 ± 13	962 ± 353	1,087 ± 321	13 ± 5
Experimental	159 ± 34*	105 ± 25*	168 ± 22*	1,898 ± 34*	1,073 ± 354	30.7 ± 20*
Adenosine						
Control	79 ± 12	40 ± 9	82 ± 9	902 ± 225	902 ± 200	10 ± 2
Experimental	71 ± 12*	37 ± 9*	84 ± 16	918 ± 227	919 ± 227	29 ± 7*
Ischemia						
Control	85 ± 17	43 ± 8	87 ± 15	909 ± 330	990 ± 238	14 ± 4
Experimental	68 ± 16*	35 ± 8*	73 ± 15*	587 ± 317*	662 ± 151*	0*

Values are means ± SD; $n = 6$. LV, left ventricle; −dP/d*t* and +dP/d*t*, rates of rise and fall, respectively, in LV pressure. *Significantly different from control ($P < 0.05$, paired *t*-test).

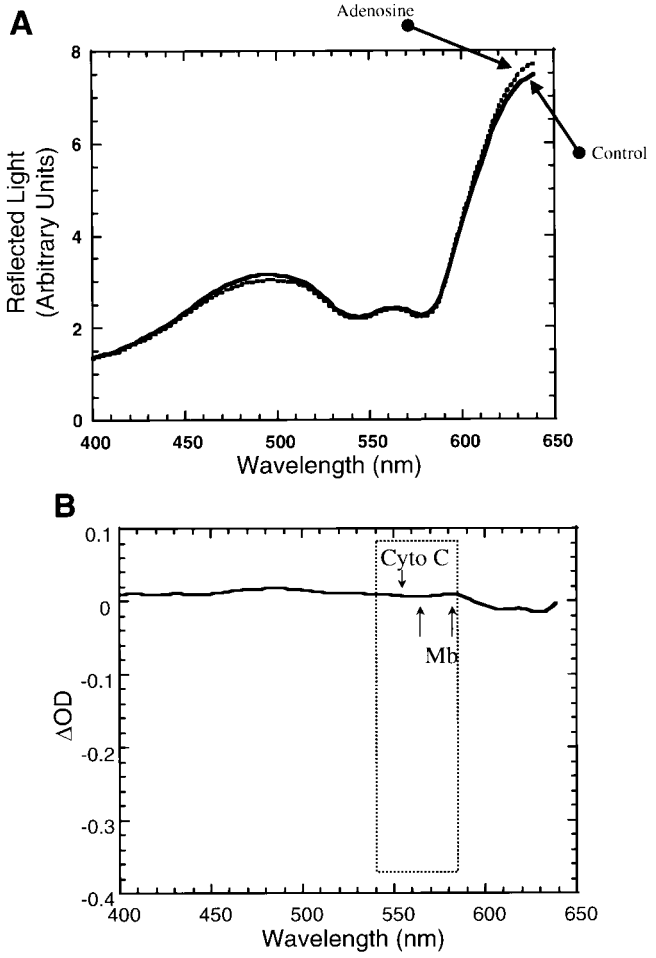

Fig. 8. Effect of adenosine infusion on porcine heart light absorption. *A*: reflected light spectrum from heart. *B*: ΔOD spectrum [log(control) − log(adenosine)] scaled to ischemia effects.

DISCUSSION

With use of a combination of a physical aperture and appropriate optics, reflection spectroscopy data were collected from the in vivo pig heart. These results were consistent with the notion that the 540- to 585-nm region of the reflected optical spectrum is dominated by cytoplasmic myoglobin and mitochondrial cytochromes. Vascular Hb O_2 saturation did not significantly influence the 540- to 585-nm region of the in vivo spectrum. The vasodilation studies suggest that the myoglobin oxygenation is high and that the myoglobin oxygenation and cytochrome *c* redox states are not affected by alterations in workload two to three times the resting anesthetized states.

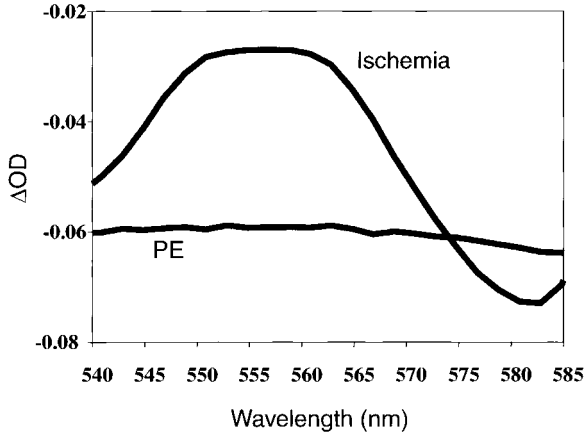

Fig. 9. Effect of phenylephrine (PE) on heart absorption. Phenylephrine data represent average of 6 experiments. ΔOD spectrum was calculated as log(control) − log(phenylephrine). Error bars were removed to simplify presentation and were on average 0.003 OD around mean. ΔOD spectrum for ischemia is provided for comparison.

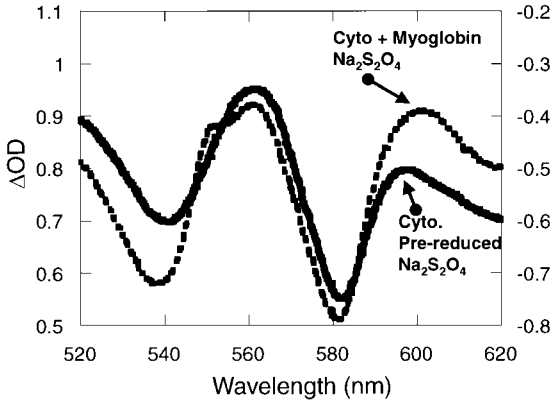

Fig. 10. Illustrative ΔOD spectra for myoglobin determination in blood-free extracts. Dotted line is ΔOD spectrum of log(control) − log($Na_2S_2O_4$) for a heart extract. Solid line is for same extract with reference cuvette treated with KCN and ascorbate to remove influence of cytochromes *c* and *a* on difference spectrum.

The hypothesis that the 540- to 585-nm band is not influenced by vascular Hb is supported by the comparison of in vitro data with in vivo spectra as well as physiological and nonphysiological manipulations in vivo. The difference spectrum between the control and ischemic heart had minima (581 nm for myoglobin) and maxima (550 nm for cytochrome *c* and 563 nm for myoglobin) similar to Hb-free tissue extract, suggesting that Hb was not significantly contributing to the difference spectrum. The 581-nm minimum is a key finding, since it differentiates between Hb and myoglobin in this spectral region. The 550-nm shoulder for cytochrome *c* clearly shows that the cytoplasmic chromophores are contributing to the reflectance spectrum. The isobestic points (545 and 558 nm) in the ischemia spectra are also consistent with the blood-free saline-perfused rabbit heart (21). Finally, all these characteristics in the 540- to 585-nm region were maintained in the ischemic difference spectrum of the blood-free pig heart. Titration of tissue extracts with blood indicates that the RBC contamination must be less than ~1% RBC to maintain an absorption minimum at 581 nm.

Beyond the maxima and minima of the spectra, the spectral shape of the in vivo ischemia difference spectrum was fit using a linear model. The model components were *1*) in vitro oxidized-reduced spectra from isolated mitochondria representing cytochromes *c* and *b* as well as oxy-deoxymyoglobin spectra from pure myoglobin or *2*) in vitro control $Na_2S_2O_4$ spectra from blood-free myocardial homogenates representing mitochondrial and cytoplasmic chromophores in the naturally occurring mole fractions. Good fits of the in vivo

data were obtained with either model. It is important to note that mitochondria and myoglobin alone could be used to fit the in vivo spectrum and that the appropriate ratio of these components, found in vivo, was maintained in the fit without including a vascular Hb component. Attempts using Hb and mitochondria models resulted in much poorer fits to the in vivo data.

These in vitro comparisons suggest that vascular Hb does not contribute to the reflected visible spectrum of the in vivo pig heart and that this region of the spectrum is dominated by cytoplasmic chromophores.

To confirm the lack of vascular Hb contribution in the 540- to 585-nm region in vivo, adenosine was used to increase the blood volume of the myocardium and to increase the mean Hb O_2 saturation by raising venous P_{O_2}. The coronary infusion of adenosine increased blood flow more than threefold (Table 1) and should have roughly doubled tissue blood volume (26, 31) and increased venous Hb saturation >70% (2). Despite these large changes in Hb content and oxygenation, adenosine infusion resulted in no specific absorption changes in the 540- to 585-nm wavelengths. Outside the 540- to 585-nm region, especially at >600 nm, alterations in the reflectance spectrum occurred that are likely the result of blood volume or O_2 saturation changes. The effects observed in the >600-nm region are consistent with the lower tissue-blood absorption in this region, leading to more blood sensitivity. Similar results were obtained in the comparison of blood-perfused and blood-free hearts (Fig. 5*B*). Previous studies have also observed spectral changes of >600 nm with ischemia in the dog heart (39) that may be caused by blood volume changes. The effects of adenosine in vivo, where induced increases in blood volume and oxygenation did not affect the 540- to 585-nm region, are consistent with a minimal influence of Hb in this region of the reflectance spectrum in vivo.

The contribution of blood to the in vivo spectral characteristics through 540–585 nm was estimated to be <0.5% of RBC volume per volume of myocardium on the basis of in vitro measures. This conclusion is consistent with the simulations of photon migration in the pig heart (15). This blood content is much lower than the values for whole heart hematocrit (i.e., RBC volume ÷ tissue volume) obtained with invasive techniques, which vary from ~2 to 9% depending on the methodology (11, 17, 32, 36). The relative insensitivity of the ischemia absorbance changes to the total tissue blood Hb may be related to the high light absorption of Hb, myoglobin, and the cytochromes at these wavelengths as well as the dynamic range of absorption changes expected for Hb. The extinction coefficient for myoglobin from 540 to 585 nm is ~2.5 times higher than at 460–510 nm and ~6–8 times higher than at 600–640 nm. Effectively, this means that the path length in the 540- to 585-nm band will be much shorter than that at wavelengths with lower absorbance. Shorter path length translates into lower probability of interaction with highly dispersed RBCs in the tissue. In addition, the RBC Hb absorption of light in this bandwidth is about two orders of magnitude higher than that of tissue. Because of this high RBC absorbance, a large fraction of photons (540–585 nm) that enter a significant blood vessel never escape for detection (15). Thus, as light enters and scatters through the myocardium, the exiting photons are highly weighted to those that only scatter through the cytosol and never encounter an RBC. A theoretical analysis of this process is presented in the companion article with use of Monte Carlo simulations and the physical data collected from the pig heart (15).

With the assumption that only the smallest vessels contribute to the spectrum, the majority of the blood detected optically will be in the capillary space. A capillary volume of 8% for the pig (45) and the lowest estimate of cardiac capillary hematocrit of 12% (38) still result in an RBC volume of ~1%, which is still above the detection threshold established in the in vitro titration experiments (Fig. 4). However, a significant fraction of heart wall blood is on the venous side of the capillary bed, where the O_2 saturation is low. Thus any further decrease in O_2 saturation with ischemia will be small relative to the entire dynamic range used in the in vitro titration. Thus a reduction in the Hb contribution by a factor of ≥2 could occur, because a large amount of Hb is not saturated with O_2 under control conditions. In the presence of adenosine the venous Hb O_2 saturation increases to ~60–70%. However, no evidence of Hb contamination was observed with subsequent ischemia in these hearts, despite the fact that the dynamic range of Hb O_2 saturation was increased. This suggests that the effect of Hb dynamic range was not dominant in determining the "visibility" of Hb in these studies. We speculate that the combination of these two effects, reduced influence of large vessels and reduced dynamic range of the venous Hb, may explain the lack of Hb contribution to the ischemic difference spectrum.

The adenosine infusion experiment also provides some insight with regard to O_2 delivery to the myocardium. Because adenosine increases the venous Hb O_2 saturation, it is assumed that the myoglobin and cytochrome redox state will trend to a more oxygenated and oxidized state, respectively, if P_{O_2} was limiting under control conditions. No changes in myoglobin or cytochrome redox state were observed with adenosine infusion. Furthermore, it has been shown that the cytochromes are highly oxidized and myoglobin fully oxygenated in the Triton X-100 tissue extracts (1). Thus the $Na_2S_2O_4$ extract vs. control difference spectrum should represent the difference between completely oxidized and reduced cytochrome as well as between oxy- and deoxymyoglobin. As shown in the model fitting, this in vitro extract difference spectrum provided a good model of the in vivo control-ischemia spectrum collected. Because ischemia should induce a near-complete reduction of the cytochromes and deoxygenation of myoglobin in vivo, it is reasonable to reach the conclusion that the agreement between the extract and in vivo difference spectra also implies that myoglobin was nearly fully oxygenated and the cytochromes

were highly oxidized. Both of these results, the adenosine effects and model fitting, are consistent with the hypothesis that the myoglobin is nearly fully oxygenated and that the P_{O_2} at the mitochondrion is in excess of that required to oxidize the cytochrome chain under control conditions. These results in the pig are similar to those of Chen et al. (7) using ^{1}H NMR to detect deoxymyoglobin in the exposed dog heart. In these NMR studies, no deoxymyoglobin was detected under control conditions with experimental limitations on the order of ±10%. These NMR data also suggest that myoglobin is nearly maximally saturated with O_2 under control conditions.

In contrast, invasive studies suggest that the mean myoglobin O_2 saturation is only ~50%. Coburn et al. (9) using ^{14}CO methods, Losse et al. (27) using O_2-sensitive electrodes, and Gayeski et al. (16) using microspectrophotometry on rapidly frozen tissue sections found that the mean heart myoglobin saturation was ~50% (P_{O_2} ~4 mmHg on the basis of affinity of myoglobin used), suggesting that O_2 could be limiting for oxidative phosphorylation in significant volumes of the tissue (9). The current optical study is not consistent with these previous studies, since no evidence for a significant amount of deoxymyoglobin or O_2 limitation to the redox state of cytochrome *c* was found. The reasons for this discrepancy between the noninvasive data (optics and NMR) and previous invasive techniques are unknown. Potentially, the fact that tissue samples were collected or electrodes were inserted into the tissue may have contributed to lower P_{O_2} values recorded with the invasive procedures.

To evaluate whether a high mean myoglobin oxygenation is physically realistic, an O_2 delivery model was developed for the in vivo pig heart. This model was derived from the work of Groebe (18) for skeletal muscle. The details of the model are presented in the APPENDIX along with the results. This three-dimensional simulation reveals that the total myoglobin O_2 saturation could be on the order of 92% (see Table 3). Simulation of the adenosine flow changes results in an increase in myoglobin saturation to 95% (see Table 3). This predicted 3% change in saturation is well within the noise of the current optical studies. Similar conclusions were found in the control state of the dog heart (see Table 4), consistent with the ^{1}H NMR data. Thus a physical model of O_2 delivery in the myocardium is consistent with the hypothesis that myoglobin O_2 saturation is >90% under control conditions.

The effect of work was evaluated to gain some insight into myocardial O_2 delivery. Increasing cardiac work with systemic infusions of phenylephrine caused no change in the myoglobin oxygenation or cytochrome *c* redox state (Fig. 9). Similar results were obtained in three studies with dobutamine or aortic constriction to increase work (not shown). These results suggest that the O_2 delivery was adequate to maintain tissue P_{O_2}, despite two- to threefold increases in O_2 consumption. This is similar to the conclusions of previous invasive studies that found the apparent muscle P_{O_2} to be constant over a wide range of flows and workloads, even though the absolute P_{O_2} was determined to be very low, as discussed above. Simulation of these workload data also reveals that the measured increases in coronary flow were adequate to maintain the total myoglobin saturation at very high levels (see Table 3). This was also true for the dog heart in vivo with use of data for near-maximal workloads (44), where large declines in myoglobin oxygenation were observed only at the highest workloads imposed (see Table 4).

Facilitated diffusion of O_2 by myoglobin depends on a gradient of oxymyoglobin in the cytosol (47). The cytosolic oxymyoglobin gradient must be small, since myoglobin is nearly completely oxygenated under control and moderate workload conditions. The combined effects of high myoglobin O_2 saturation (present study; 7), low myoglobin diffusion coefficient in muscle (23), and relatively low concentration of myoglobin in heart result in a minimal contribution of myoglobin to O_2 transport. The simulations suggest that the myoglobin contribution to O_2 transport is <1% over the entire myocardium. Myoglobin-facilitated O_2 diffusion approaches 5% in the 10% of the myocardium capillary diffusion bed farthest from entry of the arterial blood. At the workloads reached in this study and those simulated for the dog (see APPENDIX), the contribution of myoglobin to facilitated diffusion seems to be minimal in the heart until near-maximal rates of respiration are achieved. Similar conclusions were reached by Cole et al. (10) for the perfused dog heart after reduction of myoglobin facilitated diffusion with inhibitors. Myoglobin-facilitated O_2 diffusion may play a more important role at very high workloads, ischemia, or hypoxic conditions. However, under normal physiological conditions, myoglobin may serve more as a temporal buffer, reducing oscillations in tissue P_{O_2} as a result of phasic flow and metabolic activity. Funk et al. (14) proposed a similar temporal buffer role for another large cellular metabolic buffer in the heart, creatine phosphate. Thus both of these large buffer pools in the heart, oxymyoglobin and creatine phosphate, may be more important for the temporal maintenance of cellular homeostasis and not for cytosolic transport of metabolites.

The lack of change in tissue P_{O_2} with workload also implies that the gross tissue levels of O_2 are not contributing to the regulation of O_2 consumption or regional blood flow within the dynamic range of these measures. With regard to metabolism, the measures of cytochrome *c* redox state are interesting since an increase in metabolic activity in isolated mitochondria, induced by ADP or P_i increases, result in a net oxidation of cytochrome *c* (4). No evidence for modification in cytochrome *c* redox state was observed in this study with moderate increases in workload. However, the cytochrome *c* redox change associated with full transitions from rest to maximum velocity in mitochondria is only 8% (4). The moderate transitions in workload [~30% of the maximum respiratory rate (30)] made in this study should cause changes in cytochrome *c* well below the signal detection levels for this in vivo measurement.

With regard to the regulation of blood flow, the vasodilation associated with the workload challenges

was not associated with significant changes in oxymyoglobin or cytochrome *c*. These results suggest that global decreases in cellular P_{O_2}, within the sensitivity limits of these measures, are not required for increases in coronary flow induced by increases in afterload, the main phenylephrine effect. Thus a simple hypoxia feedback loop is not adequate to explain the regulation of blood flow, as has been suggested previously by many investigators (3).

One of the major limitations of this optical approach is the limited path length that samples only the epicardial region of the myocardium. In the companion article (15), the mean path length was estimated to be ~1.3 mm with a mean penetration depth of ~180 μm (400-μm mean maximum depth). The in vivo optical measure was still heavily weighted by tissue dependence on vascular supply of O_2 and not surface diffusion in this open-chest preparation, since large decreases in myoglobin oxygenation were observed with the removal of vascular O_2 supply (ischemia). This was confirmed by calculating the diffusion penetration of O_2 from the surface, with myoglobin diffusion facilitation, by using the physical parameters in the APPENDIX and the one-dimensional facilitated diffusion equation of Wyman (49). In Fig. 11, P_{O_2} is supported by surface diffusion from the epicardium at different workloads. The maximum penetration was only 40 μm. These calculations suggest that a small component of the epicardium is supported via nonvascular diffusion of O_2 in an open-chest preparation. It is important to note that the ^{1}H NMR data, which are not as critically attenuated transmurally as the optical signals, yield similar data in the intact dog heart [i.e., no detectable deoxymyoglobin under control conditions (7)].

No quantitation of myoglobin O_2 saturation or cytochrome redox state is provided. This limitation is due to the inability to reach the extremes in O_2 delivery to establish the 0 and 100% points. A regional infusion of adenosine was used in an attempt to reach maximum P_{O_2}. However, simulations (see APPENDIX) suggest that even this threefold increase in blood flow was not adequate, with the myoglobin saturation only reaching 95%. Limitations of the O_2 delivery model are outlined in the APPENDIX. We know of no way to attain fully oxidized cytochrome *c* in vivo. Even regional ischemia may not be adequate to generate complete anoxia, since surface diffusion and collateral perfusion could result in some O_2 delivery. This technology, like many nondestructive in vivo tools, is limited to directional changes by use of internal controls. However, this qualitative information can still provide useful insights into physiological regulation in vivo.

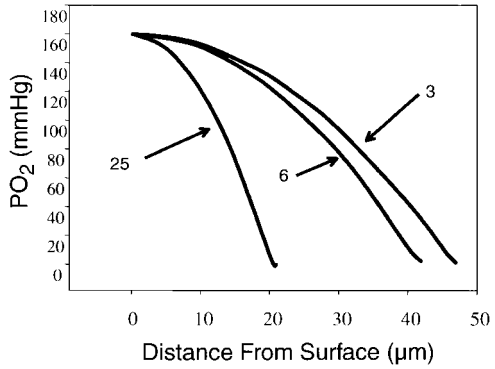

Fig. 11. Model of surface delivery of O_2 in heart. Data are presented for 3 workloads, maximum and values comparable to those used in this study (3, 6, and 25 ml·min^{-1}· 100 g tissue^{-1} O_2 consumption). O_2 diffusion and myoglobin diffusion are included using physical parameters listed in APPENDIX and 1-dimensional facilitated diffusion equation of Wyman (49).

Finally, the optical spectroscopy technology and ^{1}H NMR sampled a rather large region of the myocardium. Large gradients in myoglobin saturation or cytochrome *c* redox state could exist in small regions of the myocardium that would not be easily detected with these gross measures, as shown in the simulations. Thus conclusions of this study apply only to an average response over a ~0.8-cm^2 area of the epicardium. However, if any highly labile steep O_2 gradients do exist (22), they must not make up a significant volume of the myocardium. This restriction limits the distribution of these gradients to highly localized regions of limited total volume in the myocardium if they are going to be missed with use of these approaches.

APPENDIX

Recent quantitative data on the geometry and distribution of capillaries in the pig heart (24, 45) as well as information on myoglobin O_2 affinity (37), content (this study), and diffusion in muscle (23) provide new insights for a calculation of the mean myoglobin saturation in the pig heart in vivo. Another area of some controversy is the myoglobin concentration in the pig heart. Recent fractionation studies have suggested a pig heart myoglobin concentration of only 8×10^{-5} mol/kg (33). However, we directly determined the myoglobin content of pig hearts to be 3.6×10^{-4} mol/kg, which is more consistent with previous studies in other animal species (for examples see Ref. 48). The reason for this discrepancy is unknown.

The basic model of Groebe (18) was used for these simulations with the use of the data referred to above to modify it for heart muscle. Definitions of variables and input data are presented in Table 2. This model takes into account the RBC distribution and O_2 unloading along the capillary, O_2 diffusion in the carrier-free region (CFR) between the capillaries and tissue, and the facilitated diffusion of O_2 by Hb in the RBC and myoglobin in the muscle cell. The basic geometry for the model is shown in Fig. 12.

The model was previously described in detail by Groebe (18) for skeletal muscle. We have adapted this model to geometric and physical parameters associated with the pig and dog heart (Table 2). The first step was the calculation of the P_{O_2} at the outside of the capillary RBC [$P(z)_{RBC}$] as a function of a longitudinal coordinate (z) along the length of the capillary. This is accomplished by using the global values of capillary flow, tissue O_2 consumption, and blood O_2 content. In this model it is assumed that all the capillaries in a given region of the heart are participating in O_2 delivery. The unloading of O_2 from the RBCs follows the model of Clark et al. (8).

The diffusion of O_2 through the CFR is modeled by using the following equation at each P_{RBC} along the capillary length (z) and the radial coordinate (r) up to the myoglobin-containing

Table 2. *Physical, anatomic, and physiological parameters*

Symbol	Definition	Value
A	Capillary domain cross-sectional area	
α_{blood}	O_2 solubility of the blood	1.4×10^{-6} mol·l^{-1}·mmHg^{-1}
α_{CFR}	O_2 solubility of the CFR	9.4×10^{-7} mol·l^{-1}·mmHg^{-1}
α_m	O_2 solubility of the muscle	9.4×10^{-7} mol·l^{-1}·mmHg^{-1}
α_{RBC}	O_2 solubility of the RBC	1.5×10^{-6} mol·l^{-1}·mmHg^{-1}
C_{Hb}	Total Hb concentration in RBC	0.0203 mol/l
C_{Mb}	Total Mb concentration in heart	3.6×10^{-4} mol/l* (this study)
d_{CFR}	Thickness of CFR	1.5 μm
D_{CFR}	O_2 diffusion coefficient in CFR	1.65×10^{-5} cm^2/s
D_m	O_2 diffusion coefficient in muscle	1.16×10^{-5} cm^2/s
D_{Mb}	Mb diffusion coefficient in muscle	1.7×10^{-7} cm^2/s* (23)
D_{RBC}	O_2 diffusion coefficient in RBC	9.5×10^{-6} cm^2/s
Hct	Blood hematocrit	0.3* (pig) 0.45* (dog)
K	Rate constant of O_2 dissociation from Hb	44 s^{-1}
l	Capillary length	540 μm* (45)
l_{RBC}	RBC length in capillary	5.2 μm
P_{50Mb}	Half-saturation P_{O_2} of Mb	2.39 mmHg* (37)
$\dot{Q}_c$	Mean capillary blood flow	
r	Radial coordinate	
R_{CFR}	Radius of CFR	3.5 μm
R_{RBC}	Radius of RBC	2.0 μm
S_{RBC}	RBC surface area	65.3 μm^2
z	Longitudinal coordinate	
Cap_{RBC}	Fraction of capillary length occupied by RBC	0.15

CFR, carrier-free region; RBC, red blood cell. *Data not consistent with original use of this model for skeletal muscle (18); numbers in parentheses are reference numbers.

tissue (assumed to be 3.5 μm from the center of the capillary)

$$P_{CFR}(z, r) = P(z)_{RBC} - [\dot{V}_{O_2}(R_k^2 - R_{CFR}^2)]/(2D_{CFR}\alpha_{CFR} l_{RBC}) \ln (r/R_{RBC}) \quad (A1)$$

where P_{CFR} is P_{O_2} in the CFR, $\dot{V}_{O_2}$ is O_2 consumption, R_{CFR} is the radius of CFR, D_{CFR} is O_2 diffusion coefficient in CFR, α_{CFR} is O_2 solubility in CFR, l_{RBC} is length of RBC in capillary, and R_{RBC} is radius of RBC. This simulation resulted in a two-dimensional array $P_{CFR}(z,r)$, providing the P_{O_2} as a function of z and r in the CFR.

The effective P_{O_2} at the CFR-tissue boundary for each capillary position $[P(z)_{CFR\,limit}]$ is then used to calculate the radial P_{O_2} through the myocardium $[P_m(z,r)]$. Within the muscle, myoglobin-facilitated O_2 diffusion is included and the muscle P_{O_2} is calculated as a function of z and r as follows

$$P_{eff}(z, r) = P(z)_{CFR\,limit} + (\dot{V}_{O_2}/D_m\alpha_m)[0.5(r^2 - R_{CFR}^2) - R_K^2 \ln (r/R_{CFR})] \quad (A2)$$

$$D_F = P_{eff}(z, r) - (D_{Mb}C_{Mb}/D_m\alpha_m) - P_{50} \quad (A3)$$

$$P_m(z, r) = 0.5D_F + 0.5[D_F^2 + 4P_{eff}(z, r)P_{50}]^{0.5} \quad (A4)$$

where P_{eff} is effective P_{O_2}, D_m is O_2 diffusion coefficient in muscle, α_m is O_2 solubility of muscle, D_{Mb} is myoglobin diffusion coefficient in muscle, C_{Mb} is total myoglobin concentration in heart, and P_{50} is half-saturation P_{O_2}. D_F is an intermediate term and has no physical meaning. The muscle myoglobin saturation $[S_{Mb}(z,r)]$ was determined by numerically solving the following equation for each position in the muscle

$$S_{Mb}(z, r) = P_m(z, r)/[P_m(z, r) + P_{50}] \quad (A5)$$

Overall myoglobin saturation was determined by integrating this value over the entire muscle volume. This measure we assumed to be analogous to the measurements made by ^{1}H NMR or optical spectroscopy techniques of myoglobin O_2 saturation in vivo.

The relative contributions of O_2 (D_{O_2}) and oxymyoglobin (D_{OMb}) diffusion to the overall O_2 transport ($\dot{T}_{O_2}$) were determined using the following relationship

$$D_{OMb} = D_{Mb}C_{Mb}(\Delta S_{Mb}/\Delta r) \quad (A6)$$

$$D_{O_2} = D_{O_2}(\Delta O_2/\Delta r) \quad (A7)$$

$$\dot{T}_{O_2} = D_{OMb} + D_{O_2} \quad (A8)$$

$$F_{Mb}\dot{T}_{O_2} = 100D_{OMb}/\dot{T}_{O_2} \quad (A9)$$

where C_{Mb} is total myoglobin concentration in heart, F_{Mb} is the fraction of O_2 transport dependent on myoglobin-

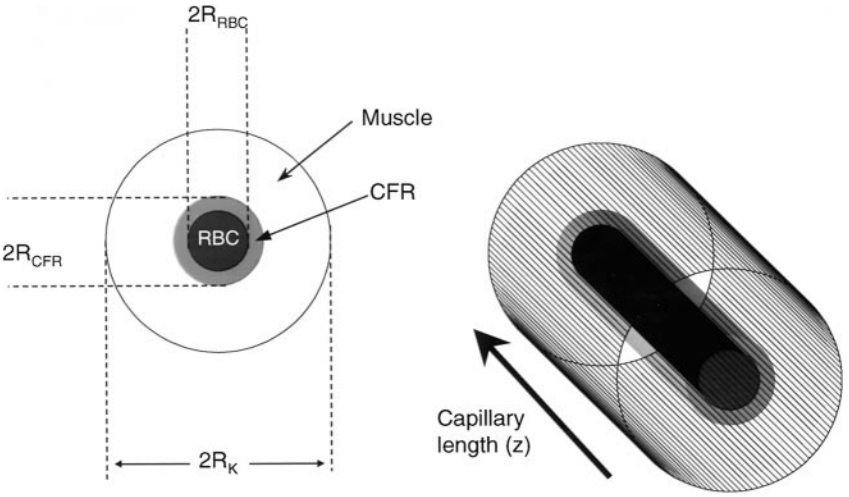

Fig. 12. Schematic model of capillary and environs. O_2 diffusion domain for capillary is shown. CFR, carrier-free region between capillary and muscle cells; R_{RBC}, radius of red blood cell/capillary; R_{CFR}, radius of CFR; R_K, Krogh radius.

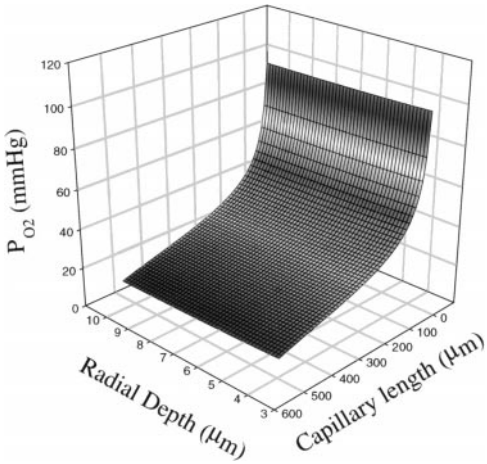

Fig. 13. Three-dimensional plot of tissue P_{O_2} as a function of position in pig heart. Data are presented along *z* and *r* spatial dimensions presented in Fig. 12. CFR and capillary zones have been removed for clarity. Plot is for control conditions in pig (see Table 3).

facilitated diffusion, and D_{O_2} is O_2 diffusion coefficient. $\dot{T}_{O_2}$, D_{O_2}, and D_{OMb} were also estimated in the regions of the lowest P_{O_2} by integrating a 10% volume of the muscle with the lowest P_{O_2}.

These equations were numerically solved for the entire capillary diffusion domain using IDL (RSI). An example of the P_m and myoglobin O_2 saturation (S_{Mb}) in the pig heart is shown in Fig. 13. The capillary and CFR regions have been excluded for clarity.

The effects of changes in cardiac perfusion and workload were modeled using the physiological parameters for control, adenosine, and phenylephrine from this study (Table 2) and for the in vivo dog described by von Restorff et al. (44) (see Table 4). No attempt to modify the functional capillary density, or Hill coefficient, with workload was made in these simulations.

Three-dimensional plots for the pig heart simulation are presented in Fig. 13 for the muscle P_{O_2} and in Fig. 14 for myoglobin O_2 saturation under control conditions. The CFR zone was omitted from Figs. 13 and 14 for clarity. Because of the high affinity of myoglobin for O_2, despite the large drop in tissue P_{O_2} down the capillary, the myoglobin remains highly

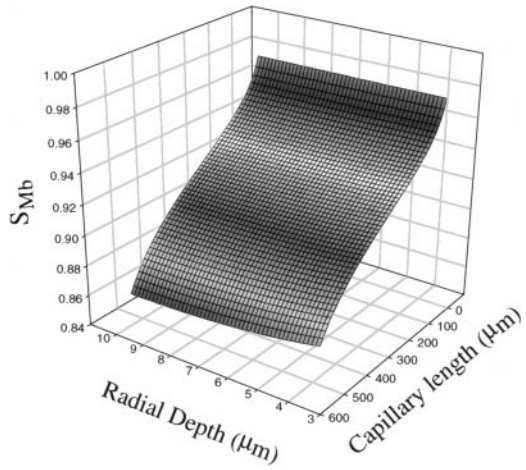

Fig. 14. Three-dimensional plot of tissue myoglobin O_2 saturation (S_{Mb}) as a function of position in pig heart. Axes are as in Fig. 13. Plot was created from same simulation generating data in Fig. 13.

Table 3. *Physiological parameters: pig from present study*

	Control	Phenylephrine	Adenosine
Coronary blood flow, ml·min^{-1}·100 g^{-1}	53	127	170
Myocardial O_2 consumption, ml·min^{-1}·100 g^{-1}	6	12	6
Overall S_{Mb}, %	91	91	94
Fractional myoglobin $\dot{T}_{O_2}$, %	<3	<3	<1
End-capillary P_{O_2}, mmHg	17	21	36
Lowest tissue P_{O_2}, mmHg	10	12	28

Overall myoglobin saturation (S_{Mb}), fractional myoglobin O_2 transport ($\dot{T}_{O_2}$), and end-capillary and lowest tissue P_{O_2} values were calculated using the model. Coronary blood flow was estimated from microsphere or left anterior descending coronary artery flow probe data.

saturated with O_2. Summaries of the data for the pig are found in Table 3. In addition to the myoglobin saturation, the end-capillary P_{O_2} is shown, which is also in good agreement with experimental values. The lowest P_{O_2} calculated was always well above the critical P_{O_2} for oxidative phosphorylation in this model. The relative contribution of myoglobin to O_2 transport over the entire muscle volume was calculated to be <3%. This is even true if it is calculated for the 10% of the tissue with the lowest tissue P_{O_2}.

Simulations were also performed for the in vivo dog; because this is a common model for cardiovascular studies, ^{1}H NMR studies have found little deoxygenated myoglobin under resting conditions, and excellent data on blood flow and metabolic rate with exercise are available. These data are summarized in Table 4. Under control and moderate workloads, myoglobin remained highly oxygenated, as observed in the pig studies and the previous ^{1}H NMR studies in dogs. Only at the highest workloads, or cardiac metabolic rates, did the total myoglobin saturation decrease markedly. At the highest workloads achieved by von Restorff et al. (44), some tissue hypoxia was predicted by the model, suggesting that O_2 limitation may be limiting performance. A similar conclusion was reached in the dog with regard to the contribution of myoglobin to O_2 transport. When the whole muscle is considered, the myoglobin contributed <1% to the O_2 transport. At the highest workloads in dogs, myoglobin supported ~20% of the O_2 transport in the 10% of the tissue with the lowest P_{O_2}.

Any simulation of complex physiological processes is limited by the inherent simplicity of the model used as well as the accuracy of the physiological, anatomic, and physical data utilized. Of particular concern in the present model are the diffusion coefficient of myoglobin and the fraction of the capillaries available for O_2 delivery as a function of workload. Furthermore, it has been shown that countercurrent flow exists in the capillaries of the heart (41). This countercurrent effect would decrease the tissue gradients even further. For

Table 4. *Physiological parameters: dog from Ref. 44*

	Control	Stage II	Stage III	Stage IV
Coronary blood flow, ml·min^{-1}·100 g^{-1}	59	129	180	224
Myocardial O_2 consumption, ml·min^{-1}·100 g^{-1}	9	24	35	47
Overall S_{Mb}, %	91	87	82	70
Fractional myoglobin $\dot{T}_{O_2}$, %	<3	6	12	19
End-capillary P_{O_2}, mmHg	22	17	16	13
Lowest tissue P_{O_2}, mmHg	14	4.8	1.2	0

these reasons and because of other limitations, this model is not accurate. However, within our current understanding of the physical and physiological parameters concerning O_2 delivery to the heart, this simulation provides some useful insights. First, the observation by both methods that myoglobin is nearly fully saturated with O_2 in the in vivo pig heart is not physically impossible. The short diffusion distances and high flow contribute to this phenomenon. Second, steep gradients in myoglobin oxygenation will not be detected by these gross measures, which integrate the entire myoglobin pool, and not selectively the regions at risk. Third, these results suggest a limited role for myoglobin in O_2 transport in the heart in vivo under control conditions because of its low concentration, small diffusion coefficient, and maintenance of relatively high P_{O_2}. Fourth, no evidence for an O_2 limitation of oxidative phosphorylation was found, except near maximum rates of work in the dog.

Address for reprint requests and other correspondence: R. S. Balaban, National Heart, Lung, and Blood Institute, National Institutes of Health, Bldg. 10, Rm. B1D416, MS 1016, Bethesda, MD 20892 (E-mail: rsb@zeus.nhlbi.nih.gov).

Received 26 February 1998; accepted in final form 22 February 1999.

REFERENCES

1. **Balaban, R. S., V. K. Mootha, and A. Arai.** Spectroscopic determination of cytochrome *c* oxidase content in tissues containing myoglobin or hemoglobin. *Anal. Biochem*. 237: 274–278, 1996.
2. **Balaban, R. S., J. F. Taylor, and R. Turner.** Effect of cardiac flow on gradient recalled echo images of the canine heart. *NMR Biomed*. 7: 89–95, 1994.
3. **Broten, T. P., J. L. Romson, D. A. Fullerton, D. M. Van Winkle, and E. O. Feigl.** Synergistic action of myocardial oxygen and carbon dioxide in controlling coronary blood flow. *Circ. Res*. 68: 531–542, 1991.
4. **Chance, B., and C. M. Williams.** The respiratory chain and oxidative phosphorylation. *Adv. Enzymol*. 17: 65–134, 1956.
5. **Chance, B., J. R. Williamson, D. Famieson, and B. Schoener.** Properties and kinetics of reduced pyridine nucleotide fluorescence of the isolated and in vivo rat heart. *Biochem. Z*. 341: 357–377, 1965.
6. **Chapman, J. B.** Fluorometric studies of oxidative metabolism in isolated papillary muscle of the rabbit. *J. Gen. Physiol*. 59: 135–154, 1972.
7. **Chen, W., J. Zhang, M. H. Eljgelshoven, Y. Zhang, X. H. Zhu, C. Wang, Y. Cho, H. Merkle, and K. Ugurbil.** Determination of deoxymyoglobin changes during graded myocardial ischemia: an in vivo ^{1}H NMR spectroscopy study. *Magn. Reson. Med*. 38: 193–197, 1997.
8. **Clark, A., W. J. Federspiel, P. A. A. Clark, and G. R. Cokelet.** Oxygen delivery from red cells. *Biophys. J*. 47: 171–181, 1985.
9. **Coburn, R. F., F. Ploegmakers, P. Gondrie, and R. Abboud.** Myocardial myoglobin oxygen tension. *Am. J. Physiol.* 224: 870–876, 1973.
10. **Cole, R. P., B. A. Wittenberg, and P. R. Caldwell.** Myoglobin function in the isolated fluorocarbon-perfused dog heart. *Am. J. Physiol*. 234 (*Heart Circ. Physiol*. 3): H567–H572, 1978.
11. **Crystal, G. J., H. F. Downey, and F. A. Bashour.** Small vessel and total coronary blood volume during intracoronary adenosine. *Am. J. Physiol*. 241 (*Heart Circ. Physiol*. 10): H194–H201, 1981.
12. **Fabel, H., and D. W. Lubbers.** Measurements of reflection spectra of the beating heart, in situ. *Biochem. Z*. 341: 351–356, 1965.
13. **French, S., P. R. Territo, and R. S. Balaban.** Correction for inner filter effects in turbid media: fluorescence assays of mitochondrial NADH. *Am. J. Physiol*. 275 (Cell Physiol. 44): C900–C909, 1998.
14. **Funk, C., A. Clark, and R. J. Connett.** How phosphocreatine buffers cyclic changes in ATP demand in working muscle. *Adv. Exp. Med. Biol*. 248: 687–692, 1989.
15. **Gandjbakhche, A. H., R. F. Bonner, A. E. Arai, and R. S. Balaban.** Visible-light photon migration through myocardium in vivo. *Am. J. Physiol*. 277 (*Heart Circ. Physiol*. 46): H698–H704, 1999.
16. **Gayeski, T. E. J., and C. R. Honig.** Intracellular P_{O_2} in individual cardiac myocytes in dogs, cats, rabbits, ferrets, and rats. *Am. J. Physiol*. 260 (*Heart Circ. Physiol*. 29): H522–H531, 1991.
17. **Gonzalez, F., and J. B. Bassingthwaighte.** Heterogeneities in regional volumes of distribution and flows in rabbit heart. *Am. J. Physiol*. 258 (*Heart Circ. Physiol*. 27): H1012–H1024, 1990.
18. **Groebe, K.** An easy-to-use model for O_2 supply to red muscle. Validity of assumptions, sensitivity to errors in data. *Biophys. J*. 68: 1246–1269, 1995.
19. **Hassinen, I. E., J. K. Hiltunen, and T. E. S. Takala.** Reflectance spectrophotometric monitoring of the isolated perfused heart as a method of measuring the oxidation-reduction state of cytochromes and oxygenation of myoglobin. *Cardiovasc. Res*. 15: 86–91, 1981.
20. **Heineman, F. W., and R. S. Balaban.** Effects of afterload and heart rate on NAD(P)H redox state in the isolated rabbit heart. *Am. J. Physiol*. 264 (*Heart Circ. Physiol*. 33): H433–H440, 1993.
21. **Heineman, F. W., V. V. Kupriyanov, R. Marshall, T. A. Fralix, and R. S. Balaban.** Myocardial oxygenation in the isolated working rabbit heart as a function of work. *Am. J. Physiol*. 262 (*Heart Circ. Physiol*. 31): H255–H267, 1992.
22. **Jones, D. P.** Intracellular diffusion gradients of O_2 and ATP. *Am. J. Physiol*. 250 (*Cell Physiol*. 19): C663–C675, 1986.
23. **Jurgens, K. D., T. Peters, and G. Gros.** Diffusivity of myoglobin in intact skeletal muscle cells. *Proc. Natl. Acad. Sci. USA* 91: 3829–3833, 1994.
24. **Kassab, G. S., and Y.-C. B. Fung.** Topology and dimensions of pig capillary network. *Am. J. Physiol*. 267 (*Heart Circ. Physiol*. 36): H319–H325, 1994.
25. **Kedem, J., A. Mayevsky, J. Sonn, and B. A. Acad.** An experimental approach for evaluation of the O_2 balance in local myocardial regions in vivo. *Q. J. Exp. Physiol*. 66: 501–514, 1981.
26. **Liu, Y.-H., R. C. Bahn, and E. L. Ritman.** Microvascular blood volume-to-flow relationships in porcine heart wall: whole body CT evaluation in vivo. *Am. J. Physiol*. 269 (*Heart Circ. Physiol*. 38): H1820–H1826, 1995.
27. **Losse, B., S. Schuchhardt, and N. Niederle.** The oxygen pressure histogram in the left ventricular myocardium of the dog. *Pflügers Arch*. 356: 121–132, 1975.
28. **Makino, N., H. Kanaide, R. Yoshimura, and M. Nakamura.** Myoglobin oxygenation remains constant during the cardiac cycle. *Am. J. Physiol*. 245 (*Heart Circ. Physiol*. 14): H237–H243, 1983.
29. **Mills, S. A., F. F. Jobsis, and A. V. Seaber.** A fluorometric study of oxidative metabolism in the in vivo canine heart during acute ischemia and hypoxia. *Ann. Surg*. 186: 193–200, 1977.
30. **Mootha, V. K., A. E. Arai, and R. S. Balaban.** Maximum oxidative phosphorylation capacity of the mammalian heart. *Am. J. Physiol*. 272 (*Heart Circ. Physiol*. 41): H769–H775, 1997.
31. **Morgenstern, C., U. Holjes, G. Arnold, and W. Lochner.** The influence of coronary pressure and coronary flow on intracoronary blood volume and geometry of the left ventricle. *Pflügers Arch*. 340: 101–111, 1973.
32. **Myers, W. W., and C. R. Honig.** Number and distribution of capillaries as determinants of myocardial oxygen tension. *Am. J. Physiol*. 207: 653–660, 1964.
33. **O'Brien, P. J., H. Shen, L. J. McCutcheon, M. O'Grady, P. J. Byrne, H. W. Ferguson, M. S. Mirsalimi, R. J. Julian, J. M. Sargeant, R. R.M. Tremblay, and T. E. Blackwell.** Rapid, simple and sensitive microassay for skeletal and cardiac muscle myoglobin and hemoglobin: use in various animals indicates functional role of myohemoproteins. *Mol. Cell. Biochem*. 112: 45–52, 1992.
34. **Parsons, W. J., J. C. Rembert, R. P. Bauman, F. G. Duhaylongsod, J. C. Greenfield, Jr., and C. A. Piantadosi.** Myocardial oxygenation in dogs during partial and complete coronary artery occlusion. *Circ. Res*. 73: 458–464, 1993.
35. **Parsons, W. J., J. C. Rembert, R. P. Bauman, J. C. Greenfield, Jr., and C. A. Piantadosi.** Dynamic mechanisms of

cardiac oxygenation during brief ischemia and reperfusion. *Am. J. Physiol*. 259 (*Heart Circ. Physiol*. 28): H1477–H1485, 1990.
36. **Rakusan, K.** Vascular capacity and hematocrit in experimental cardiomegaly due to aortic constriction in rats. *Can. J. Physiol. Pharmacol*. 49: 819–823, 1971.
37. **Schenkman, K. A., D. R. Marble, D. H. Burns, and E. O. Feigl.** Myoglobin oxygen dissociation by multiwavelength spectroscopy. *J. Appl. Physiol*. 82: 86–92, 1997.
38. **Silverman, D. A., and K. Rakusan.** Red blood cell spacing in rat coronary capillaries during the cardiac cycle. *Microvasc. Res*. 52: 143–156, 1996.
39. **Snow, T. R., L. H. Kleinman, J. C. Lamanna, A. S. Wichsler, and F. F. Jobsis.** Response of cytochrome a,a_3 in the in situ canine heart to transient ischemic episodes. *Basic Res. Cardiol*. 76: 289–304, 1981.
40. **Snow, T. R., E. Vanoli, G. De Ferrari, M. Stramba-Badiale, and D. T. Dickey.** Response of cytochrome a,a_3 to carbon monoxide in canine hearts with prior infarcts. *Life Sci*. 42: 927–931, 1988.
41. **Steinhausen, M., H. Tillmanns, and H. Thederan.** Microcirculation of the epimyocardial layer of the heart. *Pflügers Arch*. 378: 9–14, 1978.
42. **Tamura, M., N. Oshino, B. Chance, and I. A. Silver.** Optical measurements of intracellular oxygen concentrations of rat heart in vitro. *Arch. Biochem. Biophys*. 191: 18–22, 1978.
43. **Thorniley, M. S., A. Lahiri, B. Glenville, C. Shurey, G. Baker, U. Ravel, J. Crawley, and C. J. Green.** Non-invasive measurement of cardiac oxygenation and haemodynamics during transient episodes of coronary artery occlusion and reperfusion in the pig. *Clin. Sci. (Colch.)* 91: 51–58, 1996.
44. **Von Restorff, W., J. Holtz, and E. Bassenge.** Exercise induced augmentation of myocardial oxygen extraction in spite of normal dilatory capacity in dogs. *Pflügers Arch*. 372: 181–185, 1977.
45. **White, F. C., L. Nimmo, Y. Nakatani, and C. M. Bloor.** Compensatory angiogenesis during progressive right ventricular hypertrophy. *Am. J. Cardiovasc. Pathol*. 4: 51–68, 1992.
46. **Williamson, J. R., and D. Jamieson.** Metabolic effects of epinephrine in the perfused rat heart. Comparison of intracellular redox states, tissue P_{O_2}, and force of contraction. *Mol. Pharmacol*. 2: 191–205, 1966.
47. **Wittenberg, B. A., and J. B. Wittenberg.** Transport of oxygen in muscle. *Annu. Rev. Physiol*. 51: 857–878, 1989.
48. **Wittenberg, J. B.** Myoglobin-facilitated oxygen diffusion: role of myoglobin in oxygen entry into muscle. *Physiol. Rev*. 50: 559–632, 1970.
49. **Wyman, J.** Facilitated diffusion and the possible role of myoglobin as a transport mechanism. *J. Biol. Chem*. 241: 115–121, 1966.